CASE NEWS

CENTER FOR THE ADVANCED STUDY OF THE ENVIRONMENT

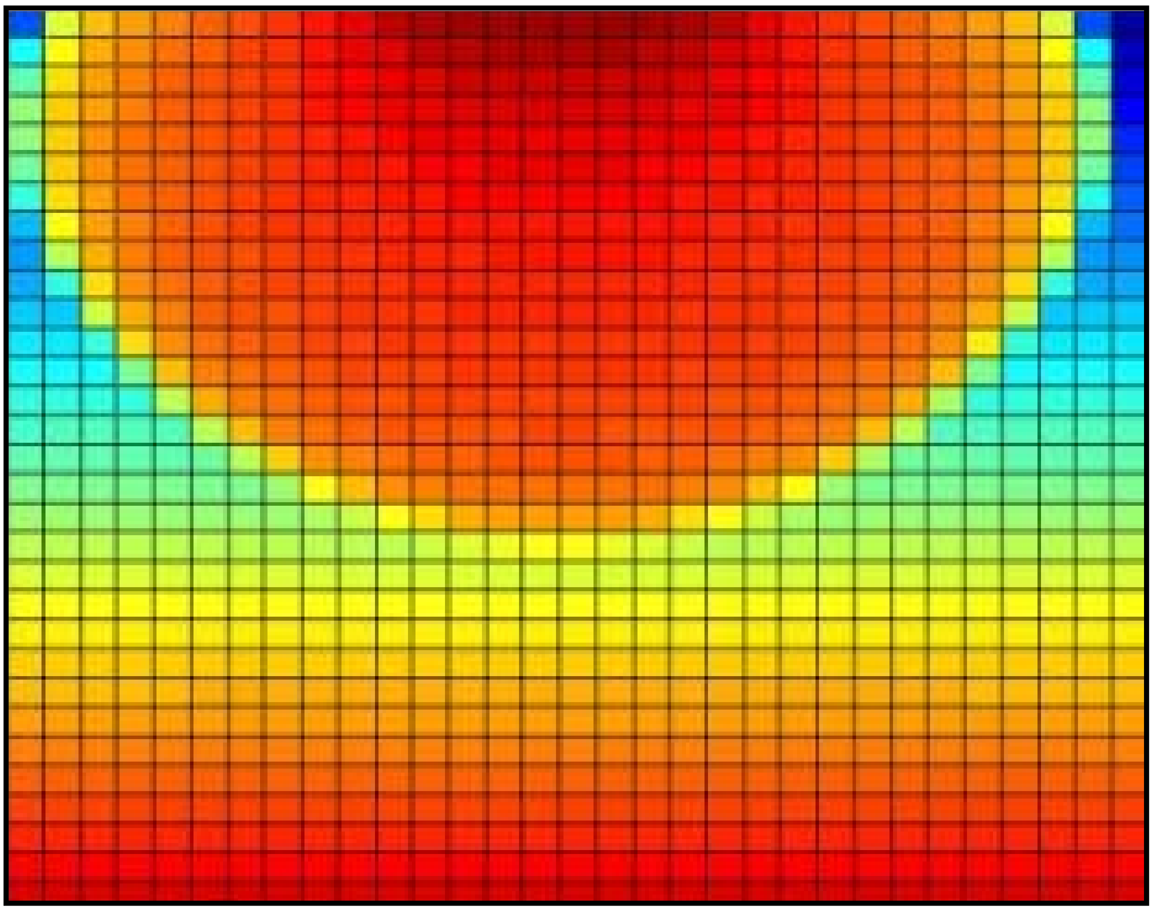

DEPARTMENT OF ENVIRONMENTAL
SCIENCES AND ENGINEERING

SCHOOL OF PUBLIC HEALTH

THE UNIVERSITY OF NORTH CAROLINA
AT CHAPEL HILL

VOLUME 1, NUMBER 1, WINTER / SPRING 2001

CASE NEWS **ISSN 1530-0528**

Department of Environmental Sciences and Engineering, School of Public Health
The University of North Carolina at Chapel Hill

Winter/Spring 2001

I am pleased to introduce this newsletter which summarizes the recent activities within the Center for the Advanced Study of the Environment (CASE). *CASE News* replaces an earlier newsletter, *CMR News*. The CASE has considerably expanded the research focus of the CMR (Center for Multiphase Research) to study the theoretical and computational modeling of spatiotemporal physical and biological systems; the investigation (through modeling and experimentation) of flow, transport and reaction phenomena in complex subsurface processes; modern geostatistics; mathematical toxicokinetics; enviroinformatics; air pollution monitoring and control; exposure analysis and health effects; risk assessment; and environmental epidemiology.

This publication will summarize a few projects in each issue with articles of intermediate length and depth of coverage. Those desiring more information may browse the web site at **http://www.sph.unc.edu/envr/case/** for a complete list of CASE personnel and publications.

George Christakos, Director, CASE

In this issue . . .

Renormalization and Upscaling Analysis: From a Grain of Sand to Complex Heterogeneities 1
A Demonstration of DNAPL Remediation Through Controlled Mobilization 9
An Investigation of Three-Phase Flow 15
Recent Work 21
Directory of the Center for the Advanced Study of the Environment 24

About the cover . . .

The cover image shows water infiltrating homogeneous porous media; the illustration was generated by solving the two-dimensional Richards' equation. The red regions indicate areas of high pressure head and thus high water saturation. The numerical solution was carried out by a CASE-developed code, which was also used for the work in "An Investigation of Three-Phase Flow," in this issue.

Renormalization and Upscaling Analysis: From a Grain of Sand to Complex Heterogeneities

by Dionissios T. Hristopulos and George Christakos

Introduction

The organization of matter and the behavior of natural processes depend to a large extent on the physical scale. Thus, even though a few fundamental laws govern all known physical interactions, an astonishing variety of phenomena emerge as natural media interact over different scales (Anderson, 1984). Questions related to scale effects abound in the environmental and health sciences (Christakos and Hristopulos, 1998a). In particular, measurements of the natural fields that determine exposure to pollutants and toxic substances are usually available at one scale, while an estimate of their effect on humans and the environment is required at a different scale. Hence, the problem of information transfer across scales is common to many environmental investigations.

More specifically, in groundwater hydrology the term “upscaling” is used to denote procedures by means of which the large-scale flow and transport properties (e.g., in a contaminated aquifer or an oil reservoir) can be inferred from the statistical information characterizing the medium at smaller scales. Physical and mathematical models of upscaling must account for heterogeneity, i.e., for the variability of natural media and processes at small scales. The term “small” refers not to a specific physical length but rather to a scale where the available data allow a statistical characterization of the medium. To avoid confusion we use the term “local” to denote this scale. Similarly, “large” is defined with reference to the local scale.

The primary challenge of upscaling procedures is to obtain large-scale representations that account for variability and uncertainty at the local scale as well as for the physical laws of flow and transport. Mathematical models are called “stochastic” when they account for heterogeneity and statistical uncertainty and incorporate them in their predictions. Figure 1 illustrates the upscaling problem.

Criticisms and Misconceptions

Critics of upscaling often ask whether it is mathematically well defined and practically feasible. Einstein once said, “the devil is in the details,” and his dictum is true in the case of upscaling as well. In modeling there are two levels of approximation: the first concerns the statistical characterization of the medium or process that leads to a specific model of heterogeneity; the second is associated with the solution of the system of equations that represent the environmental process of interest. Assuming that an accurate model of heterogeneity is obtainable from the data, upscaling estimates can be derived based on different approximations. Hence, upscaling is well defined under these constraints. For example, we can calculate the average velocity and large-scale dispersivity in porous media provided that the media properties can be locally characterized by means of probability distributions (first level of approximation). The available data for subsurface processes, however, are usually insufficient for a complete characterization (in the statistical sense) at any scale. In addition, data (e.g., permeability measurements) may have been obtained at different scales or by means of different experimental methods that involve nonuniform error sources and approximations (e.g., Neuman, 1990). Assumptions regarding the probability distribution (first level of approximation) thus cannot always be verified

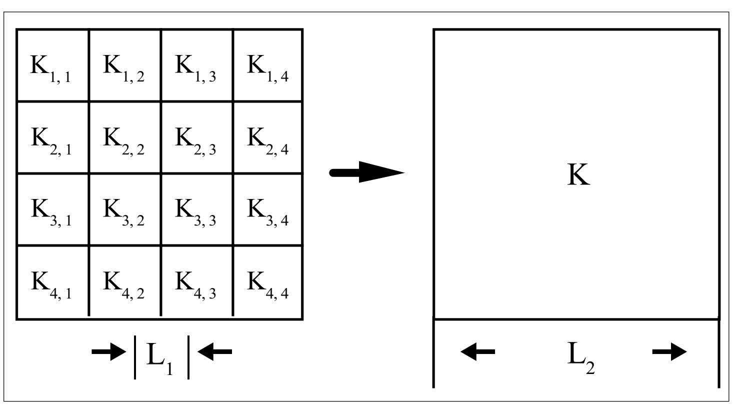

Figure 1: The upscaling question: “Given a statistical representation of the permeability at a certain scale L_1, what is the equivalent statistical representation in terms of a reduced set of variables at a scale $L_2 > L_1$?”

in practice. We believe, however, that the difficulty in verifying the statistical models should not impede the development of improved models of heterogeneity. Such models should aim to incorporate new types of variability and to improve the assumptions inherent in the second level of approximation (model solving). Even if *a priori* model justification is not feasible, *a posteriori* justification is often possible by verifying the model predictions. For risk assessment purposes, it is crucial to develop stochastic models and solution methods that accurately handle the uncertainty and variability of environmental and health processes. In addition, such models can be useful by exposing situations where variability and uncertainty conspire to prevent accurate predictions.

Some claim that all the upscaling problems in subsurface hydrology have been solved. This claim underestimates the potential of stochastic methods and the constraints imposed on existing methods by the two levels of approximation. To date, only a restrictive class of stochastic models has been investigated in the environmental sciences. These models involve assumptions that are not realistic for all media and processes of interest. In hydrology, for example, this restricted class often monopolizes the name "stochastic hydrology." Instead, we will call it the "classical hydrology approach." As we show below, stochastic models of heterogeneity span a considerably larger spectrum, and different models are appropriate for different types of media. It is crucial to realize that certain models of flow and transport lead to fundamental differences in large-scale behavior from their more thoroughly studied counterparts. An improved classification of the large-scale behavior will permit formulating different exposure scenarios and a more complete picture of the associated risk. Investigation of different scenarios is crucial, since the available data often do not specify a unique model with confidence.

Another common criticism is that upscaling methods do not work—that they do not predict field-scale behavior accurately. This claim results from two misconceptions: that a model is a set of omnipotent predictions and that stochastic upscaling is limited to the classical hydrology models. The fact is that all models involve the two levels of approximation discussed above, so testing the predictions of a model makes sense only if the underlying assumptions have first been tested and satisfied by the data. This step is often neglected by practitioners. In addition, the full scope of stochastic upscaling methods is yet undetermined, since investigations into new and exciting models of heterogeneity are still in progress. Certainly, the simplistic models which have dominated stochastic hydrology for a number of years are inadequate in most cases. If an accurate stochastic characterization is possible at some scale (first level of approximation), upscaling methods lead to accurate predictions, provided the assumptions involved in the second level are consistent with the data (e.g., Hristopulos and Christakos, 1997a, 1997b; 1999).

Upscaling research has been criticized as a scientific pursuit devoid of concrete engineering objectives. Nonetheless, upscaling has important engineering applications: numerical flow simulators cannot handle the local-scale variability of fluid permeability, and their performance can be enhanced by incorporating upscaled flow estimates at scales within the simulators' capabilities. Similar problems are faced by ocean and global climate circulation models (Cipra, 1999). In addition, performance assessment models that incorporate different elements of environmental fate and transport, exposure pathways and dose assessment require concise estimates of large-scale behavior. Such estimates can be obtained by means of upscaling methods. Finally, explicit upscaling estimates reveal general trends that characterize the relation between the local-scale heterogeneity and the large-scale behavior, without requiring time-consuming and computationally intensive calculations. Such explicit expressions can inform detailed numerical simulations conducted for specific environmental exposure situations. It is true that upscaling methods often require sophisticated mathematical analysis, especially to minimize the assumptions inherent in the second approximation level.

These methods are considered by some to be "pure science" and thus irrelevant for practical applications. Whether such focused research belongs to the realm of science or engineering is up for debate. The products of this research are nonetheless indispensable for making successful engineering and policy decisions. The fact that science and engineering are inextricably linked should not be missed: sound engineering decisions and practices are always based on good science. Sometimes political pressures and public demands require making decisions based on the best available techniques. While this leap of faith is necessary in order to address current needs for environmental policy, the need for further research to address existing scientific shortcomings should also be recognized.

a	b	c
1. Stationary permeability 2. Stationary increments	1. Normal or Lognormal 2. Heavy-tailed densities	1. Short-ranged 2. Long-ranged

Table 1: Statistical classification of heterogeneity models.

Models of Heterogeneity

The stochastic models of heterogeneity commonly used in hydrology assume normal or lognormal permeability fluctuations and short-range correlation functions; the exponential function is a common example of the latter. More general models of heterogeneity may be required to represent the local subsurface variability (e.g., Neuman, 1990; Painter, 1996; Liu and Molz, 1997). The implications of these models for the large-scale behavior of the flow field and the transport of groundwater solutes are under investigation. Different models of heterogeneity can be classified in terms of properties of the probability distribution. This can be done with respect to three properties of the multivariate distribution: a) the degree of non-stationarity; b) the distribution of the stationary variable; c) the range of the correlations between the fluctuations. Table 1 shows the results of this scheme.

A heterogeneity model can be characterized by any combination or a, b, and c. The classical stochastic hydrology deals only with the models [a1/b1/c1]. Other models in hydrology are currently being investigated: fractional Gaussian noise models [a1/b1/c2]; fractional Brownian motion models [a2/b1/c2]; and fractional Levy densities [a2/b2/c2].

The Renormalization Group Approach

The vices of the classical hydrology approach are not exclusive to the models [a1/b1/c1]: these models are solved based on strong assumptions introduced at the second level of approximation. For example, low-order perturbation methods are commonly used, restricting the validity of the calculations to weakly heterogeneous media. Better methods are required to address problems in which the restrictive assumptions are not valid.

One such method is the RG analysis that can be used to investigate the evolution of various physical parameters under change-of-scale transformations. The RG approach focuses on the entire probability distribution and not only on low-order moments (although explicit estimates for the full distribution cannot be usually obtained). As we show below, the results of RG analysis are valid for strong heterogeneity. We focus first on the fluid permeability that characterizes single-phase flow in saturated domains. In the next section we also discuss the macrodispersivity coefficient that governs the large-scale dispersion of contaminant plumes in groundwater. The sequence of transformations progressively eliminates the local fluctuations advancing from smaller scales toward larger scales. At the same time, the properties of the medium are renormalized to account for the coarse-graining of local fluctuations. Underlying the RG analysis is the idea that under the sequence of transformations a stable distribution (the “fixed point”) is approached. The fixed point distribution remains invariant under further RG transformations, and the statistical parameters of the fixed point are obtained from the RG recursion relations. In this sense, the RG is a generalization of the central limit theorems for independent random variables (Bouchaud and Georges, 1990).

The RG analysis has a wider scope than limit theorems, because the renormalized variables are correlated and the coarse-graining transformation is, in general, non-additive. King (1989) showed, using a numerical RG approach, that a uniform permeability distribution tends to a fixed point approximated by the Gaussian. In fact, the permeability fixed point is not exactly Gaussian, because the latter involves a finite weight for unphysical negative permeabilities. It is thus more likely that the permeability fixed point is an asymmetric stable distribution (e.g., Liu and Molz, 1997) that closely resembles the Gaussian but has no negative tail. Local permeability distributions, including the lognormal, that do not have significant weight in their tail lead to similar large-scale behavior. This behavior is characterized by a narrow fixed-point distribution centered on a mean that accurately determines the large-scale behavior. The mean represents the effective permeability and remains invariant under further RG transformations. The variance and other moments are continuously renormalized by the RG transformation (Hristopulos and Christakos, 1999).

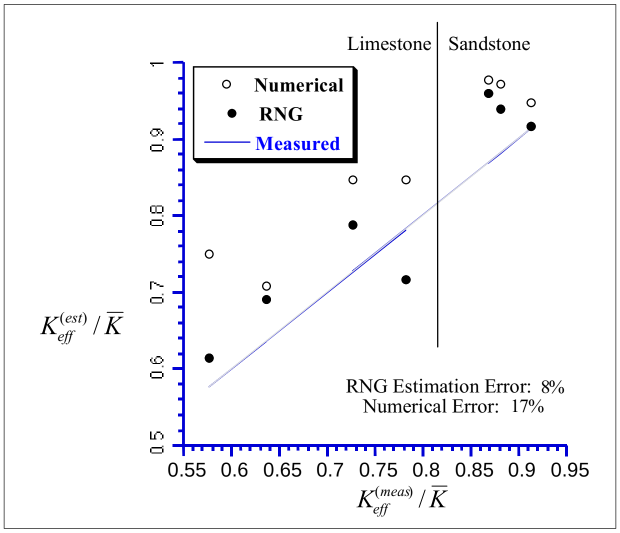

Figure 2: Plot of the effective permeabilities for limestone and sandstone. The solid circles denote the RG estimates, the open circles the numerical estimates, and the straight line the experimental measurements in (Henriette et al., 1989).

Local permeability distributions have significant tails if the probability density decreases slowly for large permeability values, e.g., as a power law. Such distributions may have a scaling fixed point that is markedly different than the Gaussian (e.g., Mandelbrot, 1998). This has serious consequences for the large-scale behavior. In particular, it implies that the mean is not an adequate measure of large-scale variability, because the distribution maintains significant density in the tail. Thus, the effective permeability is not an accurate estimator of large-scale behavior. A more useful estimator is the most likely permeability value. In the case of heavy-tailed distributions, however, a single permeability value cannot adequately represent the variability.

RG Analysis in Real and Frequency Space

Renormalization analyses can be carried out in either real space or frequency (wavector) space. Real space approaches are more intuitive, but they are based on coarse-graining transformations obtained for resistor networks (King, 1989) or other physically motivated transformations (Renard et al., 1997) that do not directly solve the flow equation. In addition, they involve numerical calculations where the cost increases with the resolution of the grid. On the other hand, frequency space approaches explicitly satisfy the flow equation and employ the stationarity assumption to derive explicit coarse-grained estimates. We have recently obtained explicit expressions for the effective permeability of media with mild-tailed densities and range correlations (Hristopulos and Christakos, 1999).

Both approaches are based on similar principles: the coarse-graining transformation is applied repeatedly, renormalizing the permeability probability density at every step. In the real space approach, the transformation eliminates fluctuations at progressively higher scales. In the frequency approach, the transformation progressively eliminates the higher frequency correlations. At every step, the eliminated fluctuations contain a narrow shell of frequencies. This technical detail is crucial, because it allows an accurate calculation of the fluctuation effects by means of perturbation methods. The RG result is accurate to all orders, however, because it incorporates contributions from all frequency shells.

In the case of lognormal media (i.e., media with normal log-permeability fluctuations), frequency-space renormalization analysis leads to the following ordinary differential equation

$$\frac{d \ln \hat{K}(q)}{dq} = c_d \sigma_f^2 q^{d-1} \tilde{p}_f(q). \qquad (1)$$

Eq. (1) characterizes the evolution of the effective permeability $\hat{K}(q)$ under the renormalization transformation. The parameter d denotes the dimension of the medium, c_d is a constant, q is the frequency of the renormalized shell (that also denotes the renormalization

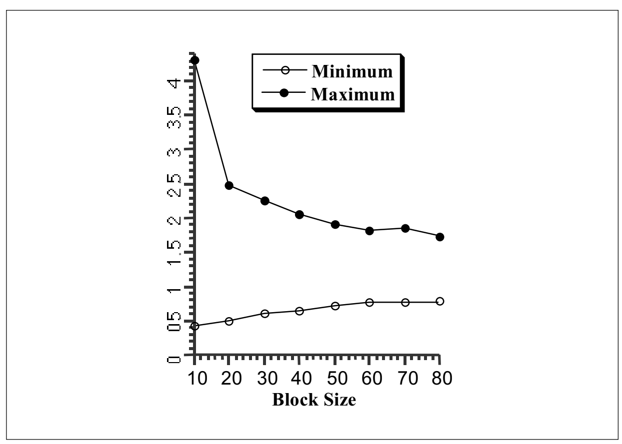

Figure 3: A plot of the minimum and maximum permeability values obtained from samples including 5,000 coarse-grained permeabilities as a function of the number of variables in the coarse-graining block.

level), $\tilde{\rho}_f(q)$ denotes the Fourier transform of the correlation function and σ_f^2 the variance of log-permeability fluctuations. For short-ranged and isotropic correlation functions the solution of Eq. (1) leads to the following expression

$$K_{eff} = \overline{K} \exp\left(-\frac{\sigma_f^2}{d}\right) \qquad (2)$$

Eq. 2 is independent of the exact shape of the correlation function and is valid in any dimension. It thus proves the Landau-Lifshitz conjecture (Landau and Lifshitz, 1980; Gelhar and Axness, 1983) in three dimensions. To our knowledge, this is the first derivation of Eq. (2) in three dimensions that accounts for all perturbation orders and does not involve any uncontrolled assumptions.

Eq. (2) has also been verified by numerical flow simulations (Neuman et al., 1992). In addition, we have recently shown (Hristopulos and Christakos 1999) that it is in excellent agreement with experimental permeability measurements in limestone (strong heterogeneity) and sandstone (weak heterogeneity). In Figure 2, we compare the RG expression with the experimental measurements and numerical estimates in Henriette et al. (1989). Note that low-order perturbation results (not shown in the picture) agree well with the sandstone data, but they fail to predict the permeability of limestone. Perturbation fails due to an insufficient second-level approximation.

Eq. (2) is equivalent to a stochastic algebraic mean in three dimensions, i.e., $K_{eff} = \langle K^{\alpha} \rangle^{1/\alpha}$ where $\alpha = 1/3$.

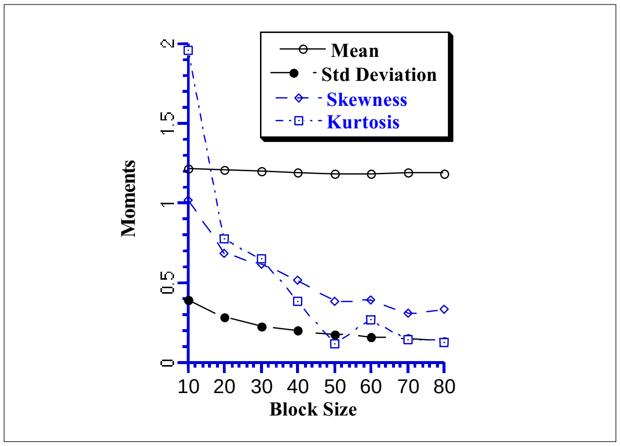

Figure 4: A plot of four statistical permeability measures (mean, standard deviation, skewness, kurtosis) obtained from samples including 5,000 coarse-grained permeabilities as a function of the number of variables in the coarse-graining block.

Assume a coarse-graining transformation in real space of the form $\overline{(K^{\alpha})}^{1/\alpha}$, where the bar denotes a sample average over a group of N variables. The permeability probability density under this transformation tends to a fixed point with mean equal to K_{eff} as N tends to infinity. This is shown schematically in Figures 3 and 4, which represent the evolution of statistical measures of the permeability distribution as the size N increases. Finally, Figures 5a and 5b show the probability density for two different block sizes N. The similarity of the two distributions agrees with the RG hypothesis.

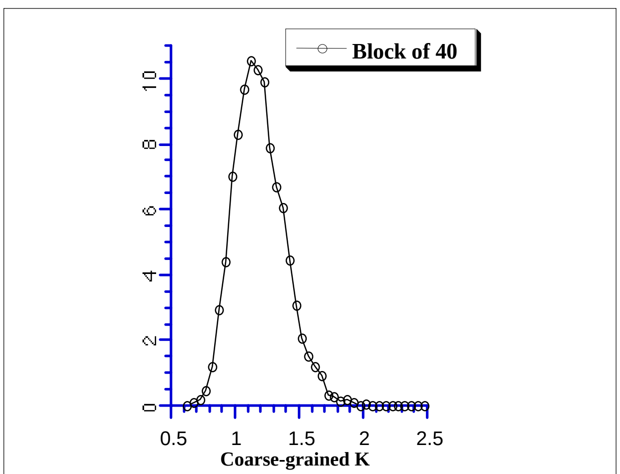

Figure 5a. Plot of the probability density for a blockcontaining 40 variables.

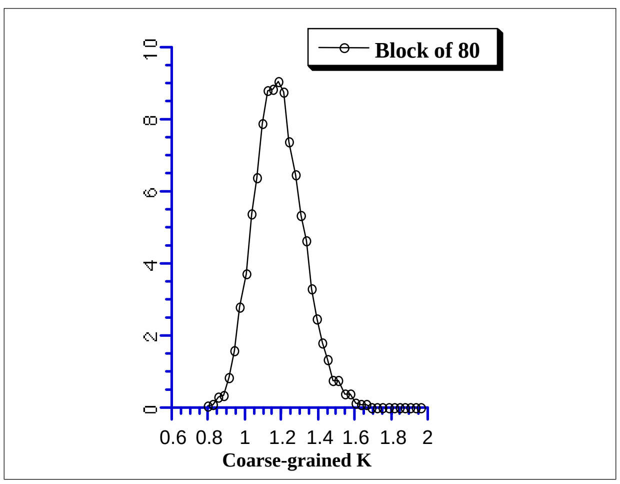

Figure 5b. Plot of the probability density for a blockcontaining 80 variables.

Renard et al. (1997) recently claimed that the algebraic mean is not an accurate predictor of the coarse-grained permeability. They reached this conclusion by calculating numerically the effective permeability of media with various probability densities and anisotropies. In such media, however, the first-level approximations of the model are not satisfied; the comparison is thus meaningless. Gelhar and Axness (1983) proposed an explicit expression for the effective permeability along the principal directions of lognormal, stratified anisotropic media:

$$K_{eff,i} = K_G \exp[-\sigma_f^2 g_i(\varepsilon)]. \tag{3}$$

Here, $g_i(\varepsilon)$ is a function that depends on the anisotropy ratio ε. Hence, the permeability in the principal directions is expressed by $K_{eff,i} = \langle K^{\alpha_i}\rangle^{1/\alpha_i}$ where the algebraic exponent is $\alpha_i = 2g_i(\varepsilon)$. A meaningful model test for anisotropic media would investigate the correctness of this result and not of its isotropic counterpart.

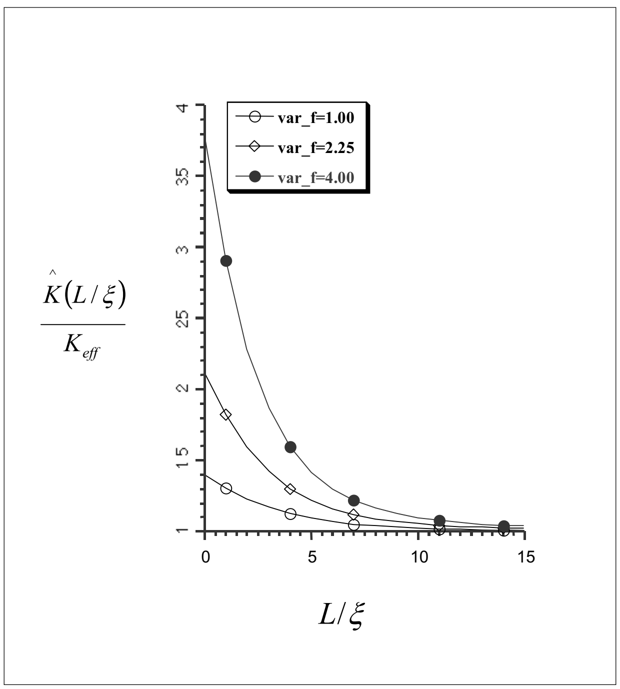

Figure 6: A plot of the effective permeability estimate (normalized by the asymptotic effective permeability) as a function of the length ratio L/ξ for three different values of the log-permeability variance σ_f^2.

In addition to Eq. (2), which is valid only asymptotically (i.e., for domains whose size significantly exceeds the correlation length) we have obtained by means of RG analysis an explicit expression for finite-size domains:

$$\hat{K}(k_c) = \overline{K} \exp\left[-\frac{\sigma_f^2}{d}\left(1 - \frac{2}{\pi}\tan^{-1}(k_c\xi) + \frac{2k_c\xi}{\pi[1+(k_c\xi)^2]}\right)\right] \tag{4}$$

L is the characteristic domain length, ξ the isotropic correlation length, and $k_c = 2\pi/L$. The above expression is valid for media with exponential permeability correlations. The function $\hat{K}(k_c)$ is plotted versus the relative separation distance L/ξ in Figure 6. For a three-dimensional domain with relative separation distance $L/\xi = 8$, Eq. (4) implies that $\hat{K}(L/\xi)$ for $\sigma_f^2 = 1$ exceeds the asymptotic value K_{eff} by 3.9%. The PAL approach (Paleologos et al., 1996) estimates the excess to be about 1.6% for the same relative separation distance and variance. For $\sigma_f^2 = 7$ and relative separation distance $L/\xi = 20$, we find that $\hat{K}(L/\xi)$ exceeds the asymptotic value K_{eff} by 2.78% compared with 9% in PAL. The predictions of both methods are remarkably close. But our approach provides an explicit expression, while the PAL approach requires the computationally intensive estimation of two infinite series of double integrals. We emphasize that if L/ξ is not large, the ergodic property does not hold (e.g., Christakos and Hristopulos, 1998b). In this case, the effective permeability is only an approximate measure of large-scale behavior.

Contaminant Transport Applications

Renormalization analysis can also be used to investigate macrodispersion, that is, the spreading of solute plumes at large distances from the source. The spreading is estimated in terms of an effective dispersion coefficient (macrodispersivity). Classical macrodispersion models severely underestimate the spreading of the plume in the transverse direction of the mean flow velocity. One possible explanation for the observed disagreement focuses on local and temporal variations of the flow field that enhance the transverse dispersion. Jaekel and Vereecken (1997) demonstrated another possibility by an RG analysis of macrodispersion: the transverse effects of heterogeneity are underestimated in the classical models due to restrictive second-level approximations.

Moreover, the classical models do not address adequately that experimental values depend on the macrodispersivity on scale (Neuman, 1990; 1994). The results of classical models are scale-independent for macrodispersivity. Implicit in this result is the Fickian behavior of the plume at large distance from the source, i.e., that the plume spreads in proportion to the square root of the travel time. Scale-dependent macrodispersivity results from anomalous, i.e., non-Fickian behavior. Several heterogeneity models in Table 1 can lead to anomalous behavior. However, a complete mathematical analysis of their effects is not available to date. An RG analysis of dispersion in disordered media has shown that anomalous behavior is obtained from normal velocity fluctuations with long-ranged correlations. In particular, if the velocity correlations in three dimensions scale at large distances as $\propto r^{-\alpha}$, where $a < 2$ is the scaling exponent, the spreading at large distance is proportional to $\propto t^{4/(2+a)}$. In this case it would appear that the macrodispersivity coefficient varies as $\propto t^{\beta}$, where $\beta = (2-\alpha)/(2+a)$ with travel time, or as $\propto L^{\beta}$ with the size of the domain.

Conclusions

Classical stochastic hydrology models lead to inaccurate predictions of large-scale environmental fluid flows due to restrictive approximations in the modeling of variability (first level) and the solution of the physical laws (second level). Renormalization analysis is a powerful tool for upscaling investigations that provides high-order accuracy. It can be used to predict the large-scale behavior of permeability and dispersivity in porous media, and it allows for the investigation of regimes of anomalous behavior inaccessible to low-order perturbation methods. Anomalous behavior is very important for an improved understanding of groundwater flow and contaminant transport at field scales. We emphasize that complex subsurface heterogeneities require a diverse arsenal of stochastic models and methods for solving flow and transport equations. Many of the methods still need to be developed. Pronouncements to the contrary notwithstanding, the book on stochastic subsurface hydrology is not yet closed. ❖

References

Anderson, P. W., *Basic Notions of Condensed Matter Physics*, Benjamin/Cummings, Menlo Park, 1984.

Bouchaud, J. P., and A. Georges, Anomalous diffusion in disordered media. Statistical mechanics, models and physical applications, *Physics Reports*, *195*, 127-293, 1990.

Christakos G., and D. T. Hristopulos, *Spatiotemporal Environmental Health Modelling: A Tractatus Stochasticus*, Kluwer, Boston, 1998a.

Christakos, G., and D. T. Hristopulos, Stochastic characterization of contaminated sites, *Journal of Applied Probability*, *34*(4), 988-1008, 1998b.

Cipra, B. A., Mathematical modelers look to an uncertain future, *SIAM News*, *31*(10), 1, 4, 1999.

Gelhar, L. W., and C. L. Axness, Three-dimensional stochastic analysis of macrodispersion in aquifers, *Water Resources Research*, *19*(1), 161-180, 1983.

Henriette, A., C. G. Jacquin, and P. M. Adler, The effective permeability of heterogeneous porous media, *Physicochemical Hydrodynamics*, *11*(1), 63, 1989.

Hristopulos, D. T., and G. Christakos, A variational calculation of the effective fluid hydraulic conductivity of heterogeneous media, *Physical Review E*, *55*(6), 7288-7298, 1997a.

Hristopulos, D. T., and G. Christakos, An analysis of hydraulic conductivity upscaling, *Proceedings of the Second World Congress of Nonlinear Analysts*, *30*(8), 4979-4984, 1997b.

Hristopulos, D. T., and G. Christakos, Diagrammatic theory of nonlocal effective hydraulic conductivity, *Journal of Stochastic Hydrology and Hydraulics*, *11*(5), 369-395, 1997c.

Hristopulos, D. T., and G. Christakos, Renormalization group analysis of permeability upscaling, *Stochastic Environmental Research and Risk Assessment 13*, 131-160, 1999.

Jaekel, U., and H. Vereecken, Renormalization group analysis of macrodispersion in a directed random flow, *Water Resources Research*, *33*(10), 2287-2299, 1997.

King, P. R., The use of renormalization for calculating effective hydraulic conductivity, *Transport in Porous Media*, *4*, 37-58, 1989.

Landau, L. D., and E. M. Lifshitz, *Statistical Physics*, Pergamon Press, Oxford, UK, 1980.

Liu, H. H., and F. Molz, Comment on “Evidence for non-Gaussian scaling behavior in heterogeneous sedimentary formations” by S. Painter, *Water Resources Research*, *33*(4), 907-908, 1997.

Mandelbrot, B., *Fractals and Scaling in Finance*, Springer Verlag, New York, 1998.

Neuman, S. P., Universal scaling of hydraulic conductivities and dispersivities in geologic media, *Water Resources Research*, *26*(8), 1749-1758, 1990.

Neuman, S. P., Generalized scaling of permeabilities: Validation and effect of support scale, *Geophysical Research Letters*, *21*(5), 349-352, 1994.

Neuman, S. P., S. Orr, O. Levin, and E. Paleologos, Theory and high-resolution finite element analysis of 2-D and 3-D effective permeabilities in strongly heterogeneous porous media, in *Mathematical Modeling in Water Resources*, Volume 2, ed. T. F. Russell, R. E. Ewing, C. A. Brebbia, W. C. Gray, and G. F. Pinder. Elsevier, New York, 118-33, 1992.

Painter, S., Evidence for non-Gaussian scaling behavior in heterogeneous sedimentary formations, *Water Resources Research*, *32*(5), 1323-1332, 1996.

Paleologos, E. K., S. P. Neuman, and D. Tartakovsky, Effective hydraulic conductivity of bounded, strongly heterogeneous porous media, *Water Resources Research*, *32*(5), 1333-1341, 1996.

Renard, P., G. LeLoc’h, E. Ledoux, and G. de Marsily, Simplified renormalization: A new quick upscaling technique, in A. Soares, J. Gómez-Hernández, and R. Froidevaux, Dordrecht, Kluwer, 89-100, 1997.

This work was supported by Grant P42 ES05948-02 from the National Institute of Environmental Health Sciences; Grant DE-FC09-93SR18262 from the Department of Energy; and Grant DAAG55-98-1-0289 from the Army Research Office.

A Demonstration of DNAPL Remediation Through Controlled Mobilization

by Edward H. Hill III, Marylène Moutier, and Cass T. Miller

Abstract

This paper describes initial laboratory investigations of a new class of controlled-mobilization remediation strategies for the removal of dense nonaqueous phase liquids (DNAPLs). These strategies are based upon density-enhanced controlled mobilization and have been developed to tackle one of the most challenging subsurface remediation problems, namely the cleanup of sites contaminated with DNAPL pools. Preliminary results demonstrate that implementations are potentially safe, rapid, and efficient: the strategy limits the extent of mobilization, can succeed with less than one pore volume flushing solution, and can achieve greater than 90% removal of the DNAPL mass contained in both pools and associated residuals. Both laboratory experiments and numerical modeling efforts are in progress to prepare these ideas for real-world systems.

Introduction

DNAPL contamination is a serious and persistent environmental problem as detailed by the U.S. EPA (Huling and Weaver, 1991; Cohen and Mercer, 1993; Guarnaccia et al., 1992) and others (Schwille, 1988; Domenico and Schwartz, 1998). Many DNAPL remediation strategies have been proposed and studied, such as pump-and-treat (PAT) (Mackay and Cherry, 1989; Bartow and Davenport, 1995), vapor extraction (VE) (McCann et al., 1994; Larkin and Hemingway, 1991), air sparging (AS) (Ahlfeld et al., 1994; Bass and Brown, 1995), in-situ biodegradation (Bio) (Alexander, 1994; Ghandi et al., 1994; Ghandi et al., 1995; Brockman et al., 1995), cosolvent flushing (CF) (Brandes and Farley, 1993; Larson et al., 1981; Roeder et al., 1996; Rao et al., 1997; Lunn and Kueper, 1997; Lunn and Kueper, 1999), surfactant flushing (SF) (Okuda et al., 1996; Pennell et al., 1996a, 1996b; Longino and Kueper, 1995; Mason and Kueper, 1996; Willson et al., 1999), steam injection (SI) (Forsyth, 1994; Sittler et al.,

Name	Formula	Temperature (deg. C)	g/100g sat. soln.	Density (*g/cc*)
ammonium iodide	NH_4I	25	64.5	1.646
barium iodide	BaI_2 - $7.5H_2O$	25	68.8	2.277
barium bromide	$BaBr_2$	20	51.0	1.710
barium perchlorate	$Ba(ClO_4)_2$	25	75.3	1.936
calcium bromide	$CaBr_2$	20	58.8	1.82
calcium chloride	$CaCl_2$-$6H_2O$	25	46.1	1.47
calcium iodide	CaI_2	20	67.6	2.125
magnesium bromide	$MgBr_2$-$6H_2O$	18	50.1	1.655
magnesium iodide	MgI_2-$8H_2O$	18	59.7	1.909
potassium chloride	KCl	25	26.5	1.178
potassium citrate	$KC_6H_5O_7$	25	60.9	1.514
potassium iodide	KI	25	59.8	1.721
sodium bisulfate	$NaHSO_4$-H_2O	25	59.0	1.47
sodium bromide	$NaBr$-$2H_2O$	25	48.6	1.542
sodium chlorate	$NaClO_3$	25	51.7	1.440
sodium chloride	$NaCl$	25	26.5	1.198
sodium iodide	NaI	25	64.8	1.919
sodium perchlorate	$NaClO_4$	25	67.8	1.683
sucrose	$Cl_2H_{22}O_{11}$	25	67.89	1.340

Table 1. Densities of selected compounds.

DNAPL	Density @ 20° C (*g*/*cc*)
carbon tetrachloride	1.59
o-dichlorobenzene	1.31
m-dichlorobenzene	1.29
1,1-dichloroethane	1.17
1,2-dichloroethane	1.26
1,1,1-trichloroethane (1,1,1-TCA)	1.35
1,1,2-trichloroethane (1,1,2-TCA)	1.44
1,1-dichloroethylene	1.22
trichloroethylene (TCE)	1.46
tetrachloroethylene (PCE)	1.63

Table 2. Densities of some common DNAPLs (Schwille, 1988).

1992), and reactive walls (RW) (Kaplan et al., 1996). All of these strategies remove DNAPL mass from laboratory columns and, in some cases, field test sites. None of them, however, has been effective for cleaning up sites containing DNAPL pools.

The problems facing current methods for the removal of DNAPL pools are primarily due to mass-transfer limitations and mobilization risks. Mass transfer limitations are very common since there are numerous physical and chemical phenomena that impede the treatment processes. The barriers to mass transfer can be physical (e.g., low hydraulic conductivities, bypassing due to heterogeneity), chemical (e.g., slow diffusion across phases, low solubilities), or both. These phenomena can result in inefficient delivery of flushing solutions (chemicals, heat, etc.), slow rates of dissolution from pools, and/or slow reaction rates.

Uncontrolled mobilization of DNAPLs is also a concern. Unlike LNAPLs, where mobilization is generally helpful, mobilization may spread DNAPLs into deeper and previously uncontaminated media. Mobilization can also result in the movement of DNAPLs into more finely grained media that are more difficult to access and remediate, so great efforts are usually made to reduce the likelihood of uncontrolled DNAPL mobilization during cleanup.

Approach

Our hypothesis for this study was that DNAPLs could be mobilized in a controlled fashion. The first implementation idea to emerge was effectively to turn the DNAPL into LNAPL by increasing the density of the surrounding aqueous phase, which can be accomplished by dissolving salts, sugars, or other additives into an aqueous phase flushing solution. As shown in Table 1, many additives can be used to achieve densities greater than the common DNAPL constituents, listed in Table 2.

This "DNAPL flotation" idea is similar to the DNAPL swelling and mobilization previously proposed by Brandes and Farley (1993) and more recently studied by others (Roeder et al., 1996; Rao et al., 1997; Lunn and Kueper, 1997, 1999). The flotation idea, however, has two theoretical advantages. First, aqueous-phase flushing solutions can be concocted in such a way that the buoyancy driving force is much stronger than can be achieved using chemical (alcohol) dilution. Second, the process does not require a potentially slow and difficult mass transfer between the aqueous and DNAPL phases.

As it became apparent that both chemistry and economics would limit the achievable aqueous-phase densities, we developed a second approach in which the density-enhanced flotation idea was used to provide a lower barrier DNAPL confinement during desaturation. By desaturating the source zone, we can achieve a density-based DNAPL mobilizing force that is on the order of three times greater than what can be achieved using many dense salt solutions. In addition to the increased density gradient, desaturation creates a more

Property	NaI Solution	TCE w/ORO	1% SDSS Solution
Composition (by weight)	60% NaI, 40% H_2O	99% TCE, 0.01% ORO	1% SDSS, 99% H_2O
Density @ 20° C (*g*/*cc*)	1.7957 ± 0.0002	1.4639 ± 0.0002	0.9987 ± 0.0002
Viscosity @ 20° C (*mPa* • *s*)	2.84	.057	0.989 ± 0.007

Table 3. Physical properties of the fluids (where "SDSS" is a 1:1 mixture of sodium diamyl- and sodium dioctyl-sulfosuccinates and "ORO" is the lypophilipc dye "Oil Red O").

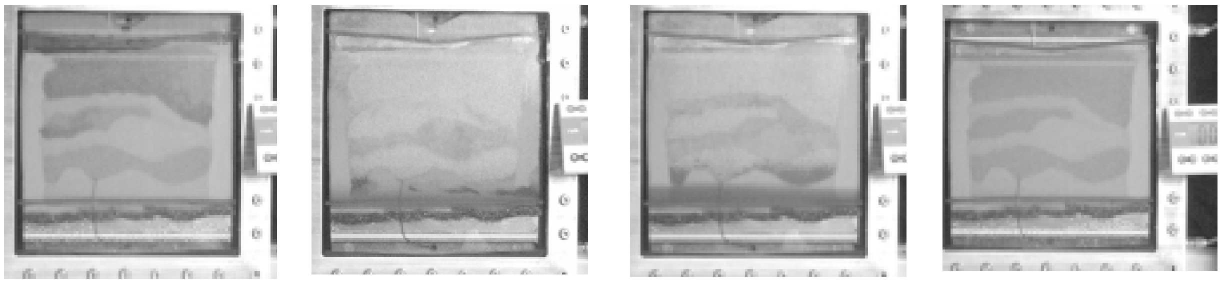

Figure 1. Demonstration of an upwards flush using a dense NaI solution.

favorable DNAPL morphology. With the introduction of a strongly non-wetting air phase, DNAPLs tend to become an intermediate-wetting film that is much more likely to flow and vaporize than the discrete blobs present within two-phase DNAPL/water systems.

Experimental Apparatus

A bench-scale experimental cell was constructed to test the new flushing strategies qualitatively. The cell was constructed of aluminum, glass, and neoprene gaskets (essentially the same as the one used by Imhoff et al. [1996]) and with internal dimensions of 20.0 ± 0.2 x 15.0 ± 0.2 x 2.0 ± 0.5 cm.

The cell was packed with three sands. A fine sand (U.S. Silica F-52, d_{50} = 0.255mm) kept the DNAPL from the neoprene gaskets. Within the remaining space, a medium sand (ASTM C-778, d_{50} = 0.347 ± 0.03mm) was used in conjunction with a coarse sand (Accusand 20/30, d_{50} = 0.713 ± 0.023mm) to create capillary barriers capable of forming DNAPL pools.

Our representative DNAPL was a 99.99%:0.01% by mass solution of trichloroethylene (TCE) and the lyphophilic dye Oil Red O. For the dense brine, a 60% by mass sodium iodide (NaI) solution was chosen. Table 3 gives the properties of these fluids.

Experimental Procedure

After creating the packing, the air in the cell was displaced with carbon dioxide. The cell was then flushed with de-aired, deionized (DDI) water to displace and/or dissolve all of the carbon dioxide gas within the porous media, giving us a domain completely saturated with DDI water. The cell was then flushed with more than ten pore volumes (>2L) of DDI water to clean (rinse) it and ensure that all gas bubbles were removed.

For both experiments, a syringe was used to inject the DNAPL (TCE w/ORO) slowly (1mL/min) into the domain. When a pool of the desired dimensions had formed, the TCE injection ceased. The TCE was allowed to reach a quasi-static fluid configuration by letting it redistribute within the domain overnight.

For the first experiment, the remediation procedure was very simple. The dense brine solution was injected into the domain from the bottom, forming a stable displacement front at a relatively slow flow rate of 1mL/min. The DNAPL minimized dynamic (viscous) effects. As predicted, the DNAPL was mobilized upward and was collected by a syringe outside the sand domain. After slightly more than one pore volume had been injected, no more DNAPL was mobilized, and a reverse flush with DDI water was performed to expel the salt solution from the domain at the same rate.

The procedure for the second experiment was more complicated. As with the first experiment, the dense NaI solution was slowly injected from the bottom of the cell. When roughly one fifth of the domain had been filled with the dense brine, the injection ceased, and the brine was left within the cell to act as a lower barrier. The top of the cell was opened to the atmosphere, and water was slowly (1mL/min) withdrawn from the lower needle to mimic the conditions of a well. The domain was slowly desaturated and the DNAPL and water collected in the syringe. After the domain had been desaturated (when the needle was withdrawing mostly air), approximately 5mL (0.3 pore volume) of a 1% surfactant solution (a 1:1

mixture of sodium diamyl- and sodium dioctyl-sulfosuccinates) was added to the top of the domain.

Results

Figure 1 shows the first experiment. The panels depict (a) the initial condition containing a TCE pool, (b) the NaI injection nearing completion, (c) the completed NaI injection, and (d) the cell following a reverse flush with DDI water that removed the NaI solution. By a direct mass balance on the TCE, 54.2% of the initial 6.510 ± 0.01g was recovered.

Figure 2 shows images from the desaturation experiment. The panels show (a) the water-saturated domain, (b) the conditions following TCE injection and pool formation, (b) the completion of the initial desaturation (before addition of the surfactant solution), and (d) the conditions following addition of the surfactant and subsequent withdrawal of mobilized TCE and water. Unfortunately, TCE losses due to evaporation and absorption by plastic tubing made impossible a direct mass balance on the extracted TCE. From visual analysis, we estimate that more than 90% of the TCE was removed from the domain.

Discussion

These results are encouraging, and they clearly demonstrate that controlled-mobilization strategies are capable of removing DNAPL pools safely and rapidly. This is a major advance over competing technologies, which are either highly inefficient or impractical for remediation scenarios containing DNAPL pools. From these initial discoveries, we can see that (1) density-enhanced approaches can remove a significant fraction of the DNAPL present in pools; (2) density-enhanced approaches can accomplish rapid removal, since only one pore volume (or less for desaturation strategies) of flushing solution is required; and (3) while capillary trapping may limit the effectiveness, the addition of a surfactant can drastically reduce trapping and result in a much higher percent removal.

We are currently working to develop techniques, both through laboratory experiments and computer modeling, that will allow us to apply these findings to field sites. ❖

References

Ahlfeld, D., A. Dahmani, G. Hoag, M. Farrel, and W. Ji, Field measurements of sparging trench in a Connecticut site: Results and comments, in *Proceedings of the Petroleum Hydrocarbons and Organic Chemicals in Ground Water: Prevention, Detection, and Remediation*, Ground Water Publishing Company, Dublin, OH, 175-190, 1994.

Alexander, M., *Biodegradation and Bioremediation*, Academic Press, San Diego, 1994.

Bartow, G., and C. Davenport, Pump-and-treat accomplishments: A review of the effectiveness of ground water remediation in Santa Clara Valley, California, *Ground Water Monitoring and Remediation, 15*(2), 140-146, 1995.

Bass, D. H., and R. A. Brown, Performance of air sparging systems—A review of case studies, in *Proceedings of the 1995 Petroleum Hydrocarbons and Organic Chemicals in Ground Water: Prevention, Detection, and Remediation*, Ground Water Publishing Company, Dublin, OH, 621-636, 1995.

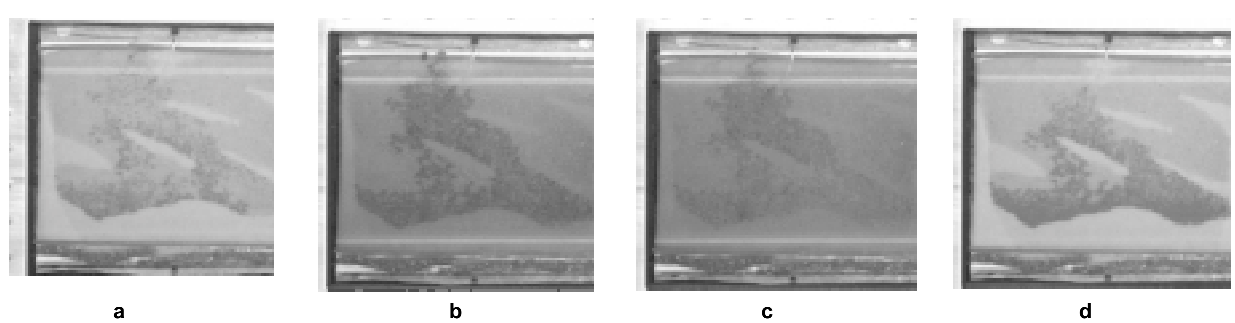

Figure 2. Demonstration of desaturation with a lower barrier composed of a dense NaI solution.

Brandes, D., and K. J. Farley, Importance of phase behavior on the removal of residual DNAPLs from porous media by alcohol flooding, *Journal of Water Environment Research, 65*(7), 869-878, 1993.

Brockman, F. J., W. Payne, D. J. Workman, A. Soong, S. Manley, and T. C. Hazen, Effect of gaseous nitrogen and phosphorus injection on in situ bioremediation of a trichloroethylene contaminated site, *Journal of Hazardous Materials, 41*(2-3), 287-298, 1995.

Cohen, R. M., and J. W. Mercer, DNAPL site evaluation, *Technical Report EPA/600/SR-93/022*, US EPA Robert S. Kerr Environmental Research Laboratory, Ada, OK, 1993.

Domenico, P. A., and F. W. Schwartz, *Physical and Chemical Hydrogeology*, Wiley, New York, 1998.

Forsyth, P. A., Three dimensional modelling of steam flush for DNAPL site remediation, *International Journal for Numerical Methods in Fluids, 19*(12), 1055-1081, 1994.

Gandhi, P., L. E. Erickson, and L. T. Fan, A simple method to study the effectiveness of bioremediation aided, pump and treat technology for aquifers contaminated by non-aqueous phase liquids, 1. Single component systems, *Journal of Hazardous Materials, 39*(1), 49-68, 1994.

Gandhi, P., L. E. Erickson, and L. T. Fan, A simple method to study the effectiveness of bioremediation aided, pump and treat technology for aquifers contaminated by non-aqueous phase liquids, 2. Multi-component systems, *Journal of Hazardous Materials, 41*(2-3), 185-204, 1995.

Guarnaccia, J. F., P. T. Imhoff, B. C. Missildine, M. Oostrom, M. A. Celia, J. H. Dane, P. R. Jaffé, and G. F. Pinder, Multiphase chemical transport in porous media, *Technical Report EPA/600/S-92/002*, US EPA Robert S. Kerr Environmental Research Laboratory, Ada, OK, 1992.

Huling, S. G., and J. W. Weaver, Dense nonaqueous phase liquids, *Technical Report EPA/540/4-91-002*, EPA Robert S. Kerr Environmental Research Laboratory, Ada, OK, 1991.

Imhoff, P. T., G. P. Thyrum, and C. T. Miller, Dissolution fingering during the solubilization of nonaqueous phase liquids in saturated porous media, 2. Experimental observations, *Water Resources Research, 32*(7), 1929-1942, 1996.

Kaplan, D. I., K. J. Cantrell, T. W. Wietsma, and M. A. Potter, Retention of zero-valent iron colloids by sand columns: Application to chemical barrier formation, *Journal of Environmental Quality, 25*(5), 1086-1094, 1996.

Larkin, R. G., and M. P. Hemingway, Results of a soil vapor extraction pilot test in low permeability terrace deposits, Kelly A.F.B., Texas, in *Proceedings of the 1991 Petroleum Hydrocarbons and Organic Chemicals in Ground Water: Prevention, Detection, and Restoration*, 191-204, Houston, TX, November 20-22, 1991.

Larson, R. G., H. T. Davis, and L. E. Scriven, Displacement of residual nonwetting fluid from porous media, *Chemical Engineering Science, 36*, 75-85, 1981.

Longino, B. L., and B. H. Kueper, The use of upward gradients to arrest downward dense, nonaqueous phase liquid (DNAPL) migration in the presence of solubilizing surfactants, *Canadian Geotechnical Journal, 32*, 296-308, 1995.

Lunn, S. R. D., and B. H. Kueper, Removal of pooled dense, nonaqueous phase liquid from saturated porous media using upward gradient alcohol floods, *Water Resources Research, 33*(10), 2207-2219, 1997.

Lunn, S. R. D., and B. H. Kueper, Risk reduction during chemical flooding: Preconditioning DNAPL density in situ prior to recovery by miscible displacement, *Environmental Science & Technology, 33*(10), 1703-1708, 1999.

Mackay, D. M., and J. A. Cherry, Groundwater contamination: Pump-and-treat remediation, *Environmental Science & Technology, 23*(6), 630-636, 1989.

Mason, A. R., and B. H. Kueper, Numerical simulation of surfactant-enhanced solubilization of pooled DNAPL, *Environmental Science & Technology, 30*(11), 3205-3215, 1996.

McCann, M., P. Boersma, J. Danko, and M. Guerriero, Remediation of a voc-contaminated Superfund site using soil vapor extraction, groundwater extraction, and treatment—A case study, *Environmental Progress, 13*(3), 208-213, 1994.

Okuda, I., J. F. McBride, S. N. Gleyzer, and C. T. Miller, An investigation of physicochemical transport processes affecting the removal of residual DNAPL by nonionic surfactant solutions, *Environmental Science & Technology, 30*(6), 1852-1860, 1996.

Pennell, K. D., L. M. Abriola, and L. E. Loverde, The use of surfactants to remediate NAPL-contaminated aquifers, in *Non-Aqueous Phase Liquids (NAPLs) in the Subsurface Environment: Assessment and Remediation*, ed. L. N. Reddi, American Society of Civil Engineers, New York, 221-232, 1996a.

Pennell, K. D., G. A. Pope, and L. M. Abriola, Influence of viscous and buoyancy forces on the mobilization of residual tetrachloroethylene during surfactant flushing, *Environmental Science & Technology, 30*, 1328-1335, 1996b.

Rao, P. S. C., M. D. Annable, R. K. Sillan, D. Dai, K. Hatfield, W. D. Graham, A. L. Wood, and C. G. Enfield, Field-scale evaluation of in situ cosolvent flushing for enhanced aquifer remediation, *Water Resources Research, 33*(12), 2673-2686, 1997.

Roeder, E., S. E. Brame, and R. W. Falta, Swelling of DNAPL by cosolvent flooding to allow its removal as an LNAPL, in *Non-Aqueous Phase Liquids (NAPLs) in the Subsurface Environment: Assessment and Remediation*, ed. L. N. Reddi, American Society of Civil Engineers, New York, 333-344, 1996.

Schwille, F., *Dense Chlorinated Solvents in Porous and Fractured Media*, Lewis, Chelsea, MI, 1988.

Sittler, S. P., G. L. Swinford, and D. G. Gardner, Use of thermal-enhanced soil vapor extraction to accelerate remediation of diesel-affected soils, in *Proceedings of the 1992 Petroleum Hydrocarbons and Organic Chemicals in Ground Water: Prevention, Detection, and Restoration*, The American Petroleum Institute and The Association of Ground Water Scientists and Engineers, 413-426, Houston, TX, November 4-6, 1992.

Willson, C. S., J. L. Hall, P. T. Imhoff, and C. T. Miller, Factors affecting bank formation during surfactant-enhanced mobilization of residual NAPL, in review, 1999.

This work was supported by Grant 5 P42 ES005948-07 from the National Institute of Environmental Health Sciences. The authors wish to thank Simon Gleyzer and John McBride for assistance with some of the measurements.

An Investigation of Three-Phase Flow

by Clinton S. Willson and Christopher E. Kees

Introduction

Transport and entrapment behavior of nonaqueous phase liquids (NAPLs) in soils depend on the distribution and interaction of three fluid phases—water, NAPL, and air. Assessment and remediation efforts directed at subsurface NAPLs rely on field data and/or numerical models. Unfortunately, reliable data is scarce at most contaminated sites, thus increasing the importance of and reliance on models. Accurate modeling of three-fluid-phase flow requires knowledge of the functional relationships among air, water, and NAPL pressures, saturations, and permeabilities (i.e., pSk relations). In addition, these relations all depend on system history (i.e., hysteresis). While functional relationships have been developed to account for these phenomena, little data exists to support their accuracy, particularly in dynamic systems. Hence, the goals of this work are to gather high-quality data and to use this data to evaluate the existing constitutive models.

In this article we present preliminary results concerning a series of NAPL infiltration experiments in a 90-cm column where an X-ray attenuation system was used to provide high-quality static and dynamic measurements of physical properties and phase saturations at various locations within the column.

Materials

The experimental column was a 90-cm chromatographic column with a 2.5 cm inner diameter. The top of the cell was open to the atmosphere, while the bottom of the column was fitted with a modified Teflon plunger. As shown in Figure 1, the plunger was fitted with a glass frit and a #60 mesh screen, each leading into separate compartments. The lower air entry pressure of the mesh screen allowed for easy movement of air ahead of the NAPL front and out the column into the atmosphere—this was vital for maintaining atmospheric pressure conditions ahead of the front during infiltration. The higher air entry pressure of the glass frit ensured the connectivity of the aqueous phase, so any water pushed ahead of the front exited the column and did not block the air pathway. Each of the compartments was attached via Teflon tubing to a three-way Swagelok fitting. A syringe infusion pump (model 22, Harvard Apparatus, South Natick, MA) connected to the Swagelok fitting at the bottom of the column, was used to saturate the media. During the drainage and pressure-saturation portions of the experiments, a constant head device was connected to the Swagelok fitting.

Deionized (DI) water was obtained from a Dracor water purification system (model 21RC1, Dracor Water Systems, Inc., Durham, NC). Soltrol 220 (Phillips Petroleum, Bartlesville, OK) was selected as the representative NAPL for all experiments. The NAPL mixture was dyed with Oil Red O (0.32 gm/L) to permit visual observation. Because water and Soltrol have very similar X-ray attenuation properties, the measurement resolution using X-rays is poor between these compounds. The resolution can be improved by adding a contrasting agent to one or both of the liquids (i.e., "doping" the liquid). Because true two-phase measurements were required (the air phase was determined via a mass balance), we doped both liquids. Following Oak et al. (1990) and McBride and Miller (2000a, 2000b), we used iodobenzene and CsCl because of their different attenuating characteristics—iodine is a good contrasting agent in the 35 keV energy range, while Cs is suitable in the 45 keV range. 1-Iodobenzene (Aldrich Chemicals) was added to the Soltrol at 2.5% by weight in order to increase the attenuation properties of the NAPL phase and yet keep the NAPL lighter than water. CsCl was added at 2.5% by weight to the DDI water.

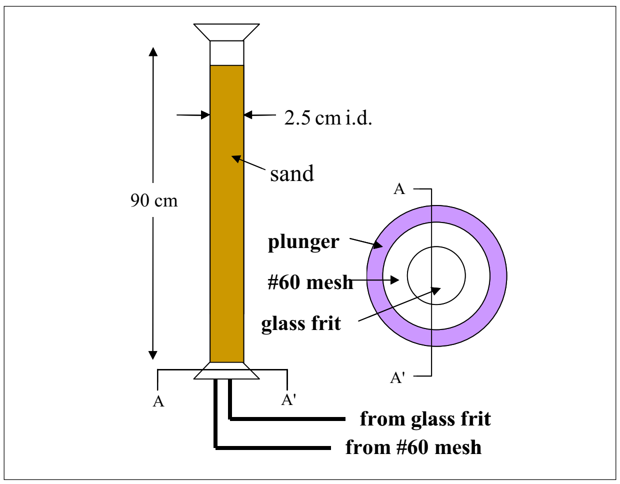

Figure 1: Experimental column and end-fitting.

	20/30 Accusand[1]	F-52[2]
Particle diameter, d50 [mm]	0.713	0.26
Ui ,d60/d10 [-]	1.190	1.59
Particle sphericity	0.9	1.01
Particle density [gm/cc]	2.664	2.654
static VG α (dr) [1/cm]	0.0679	0.0244
static VG n (dr)	13.1	11.2
K_s [cm/min]	8.94	1.2

[1] Schroth et al., 1996 [2] Hemmer, 1995

Table 1: Porous media properties.

Two different unconsolidated porous media were used in this work. The 20/30 Accusand (Unimin Corp., Le Sueur, MN) is a coarse sand that was the subject of an extensive characterization (Schroth et al., 1996). The F-52 sand (US Silica, Ottawa, IL) is a well-characterized medium-grade sand (Hemmer, 1995). Table 1 lists some of the physical properties of these sands.

The X-ray instrument comprises 160-kVp X-ray generator (Pantak Electronics), a germanium detector (EG&G ORTEC), spectroscopy electronics, and a multichannel analyzer (EG&G ORTEC). The detector and associated electronics are attached to a PC for data storage and analysis. The X-ray tube and detector move on a two-dimensional scanning system consisting of Thompson linear rails and Compumotor stepper motors.

Physical Properties

The density of the Soltrol was measured using a density meter (model DMA 48, Anton Paar, Graz, Austria). Three independent samples were measured at a given temperature. Viscosity was measured in triplicate with a falling ball viscometer (Haake Instruments, Paramus, NJ) equipped with a jacketed glassware water bath (series 9500, PolyScience Co., Niles, IL). The interfacial tension between the Soltrol and de-ionized water was measured using a drop-volume tensiometer (DVT-10, Kruss, Charlotte, NC).

Column Packing

Before packing, the column was rinsed with Methanol, washed with soap and a coarse brush, and flushed repeatedly with DDI water. The column was aligned vertically and a 1-mm layer of Wagner sand/gravel, (WG2, sieved to 0.7-1.0 mm) was poured on the bottom plunger. A 1-m long tube with a funnel on one end and a diffuser on the other was used to pour the sand into the column, which was filled by continually raising the filling tube to maintain a 5-cm gap between the diffuser and the sand surface. While filling, the column was vibrated to ensure uniform packing of the particles. The mass of sand poured into the column and the packing height were recorded in order to obtain the average porosity of the packing. A 1-mm layer of WG2 sand/gravel was then placed on the top sand surface to inhibit disruption of the surface media during the experiment. The X-ray was then used to verify that the column was vertical.

The next step was to X-ray vertically along the column centerline in the absence of any fluid phase. A series of at least 5 scans was made at 1-cm increments over the entire sand-filled portion of the column (a procedure hereafter called the "dense scan"). This data served as the point to which all subsequent X-ray measurements were compared.

Before saturating the media with water, approximately two to three pore volumes of CO_2 were injected into the cell from the bottom, followed by the injection of heated, deionized, deaired water into the column at a rate approximately equal to the saturated hydraulic conductivity of the sand. The column was flushed until no gas bubbles were visible along the column walls. After water saturation, another dense scan was performed.

The next step was to X-ray multiple locations while draining the column—this step was to obtain dynamic saturation data that would help us determine aqueous-phase pSk parameters (the "dynamic" parameters). Drainage was accomplished by connecting the bottom of the column to a constant head device placed at a specified elevation. After an initial X-ray scan of the water-saturated column, the fitting valve was opened, and water was allowed to drain out of the column through the constant head device. The column was scanned at multiple locations during the water drainage.

After the water had drained to an "equilibrium" state (~ 48 hours), another dense scan was performed. This scan provided "static" data that could be used to determine pressure-saturation parameters. Once the scanning was complete, both plunger compartments were open to the atmosphere, and water drained out of the column. After allowing for the water content to come to "equilibrium" (~ 48 hours), the column was once again densely scanned with the X-ray, allowing us to determine the initial aqueous phase content conditions for NAPL infiltration.

The NAPL weight was recorded before and after the NAPL was released onto the sand surface, providing an accurate estimate of the volume of NAPL introduced. An X-ray scan of the column was made before the NAPL was spilled. The NAPL was released just prior to the start of the second scan by pouring the liquid through a funnel that extended down to the sand surface. The time was recorded at the beginning and ending of ponded conditions. The X-ray measurements during the NAPL infiltration and redistribution consisted of two stages. The first stage was a scan over only the upper 40 cm of the column and was designed to capture as much of the flow dynamics as possible (i.e., capture the front passing a location and the beginning of the redistribution). After the NAPL front infiltrated below the 40-cm depth, the second X-ray scanning program was started—this stage was a long-duration scan at 10-cm increments over the entire column.

Both moving and still images were recorded during the NAPL infiltration experiments: the images were captured using a CCD camera (Nikon, USA) connected to a videocassette recorder and a PC running Optimus software. Following NAPL redistribution, a dense scan of the column was performed to determine the final distribution of the NAPL and the water.

X-ray attenuation methods

X-ray attenuation measures differences in the mass of one or more materials or phases. Thus the scans performed before and after fluid infiltration must be compared in order to obtain fluid content values. Unlike a natural-source device, the X-ray device can measure multiple phases and can optimize or tune the system to the problem at hand. Details of our X-ray device and path-length estimators can be found elsewhere (McBride and Miller, 1994; McBride and Miller, 2000a, 2000b; Hill, 1997). In short, the estimation methods employed in this study are aimed at extracting the maximum information from each X-ray scan. Estimator techniques include least-squares and maximum-likelihood methods (Hill, 1997).

Numerical Modeling

The mathematical models we used to simulate these experiments were the pressure head form of Richards' equation for the initial air/water system and a simplified system of three-phase flow equations for the NAPL infiltration and redistribution. We used the standard multiphase version of Darcy's law, the Mualem saturation-permeability relation, and the Van Genuchten pressure-saturation relation to close the model equations (Bear, 1972). The model equations were solved numerically using a method of lines/differential-algebraic equation (MOL/DAE) approach, which has been implemented in several codes at the CASE (Kelley, 1998, http://www.sph.unc.edu/envr/case/Codes.html).

To simulate the experimental system, we first obtained the physical parameters that are required by the model equations. We assumed that physical parameters were homogeneous throughout the column, since the sand pack was constructed to be homogeneous. The near-constant porosity data further supports the homogeneity assumption. We used the mean of the measured porosity values as the porosity of the column and then fitted the permeability and Van Genuchten parameters to the data from the water drainage portion of the experiment. The parameters were fitted by minimizing the nonlinear function given by the square of the difference in experimental and predicted values at each measurement location and time. For the minimization, we used a modified Levenberg-Marquardt algorithm implemented in the MINPACK package (Garbow et al., 1980).

The parameters for the remaining portions of the experiment will be determined by two means: extending the drainage parameters above, using empirical and theoretical relations between two- and three-phase model parameters and by fitting the full set of parameters to the experimental data, using the methods outlined above.

Results

Table 2 gives the density and viscosity of the iodoheptane/Soltrol (iodosoltrol) and CsCl/water (CsClwater) mixtures. A plot of the mass attenuation coefficient versus keV for both the doped and un-doped liquids is shown in Figure 2. We see that the attenuation peak of the iodosoltrol combination is at a lower energy than that of the CsClwater, which allows us to differenti-

	Iodosoltrol[1]	CsClwater[2]
ρ @ 20°C [gm/cc]	0.8128	1.0172
ρ @ 22.5°C [gm/cc]	0.811	1.0166
μ @ 20°C [cps]	4.44	1.0644
μ @ 22.5°C [cps]	4.11	1.0014

[1] Soltrol 220 with 2.5% by weight Iodoheptane
[2] Water with 2.5% by weight CsCl

Table 2. Fluid Properties

Figure 2

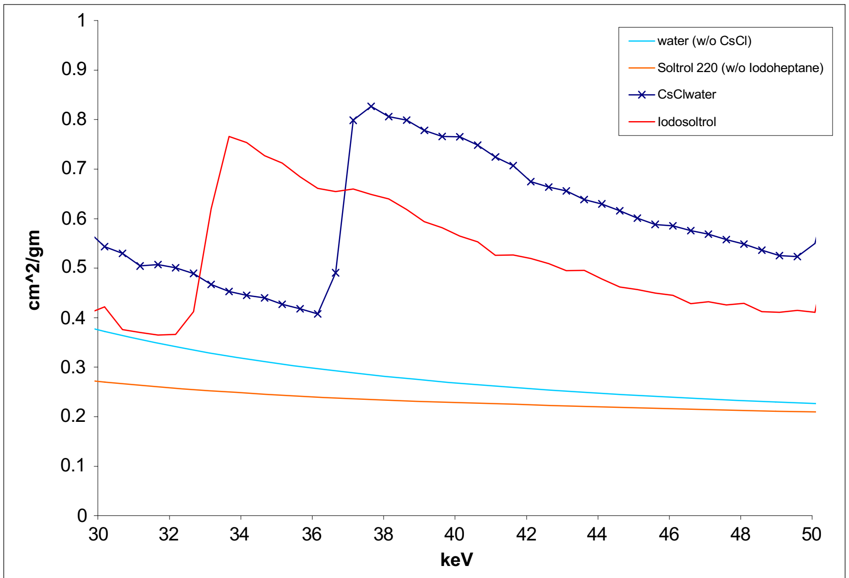

Figure 3

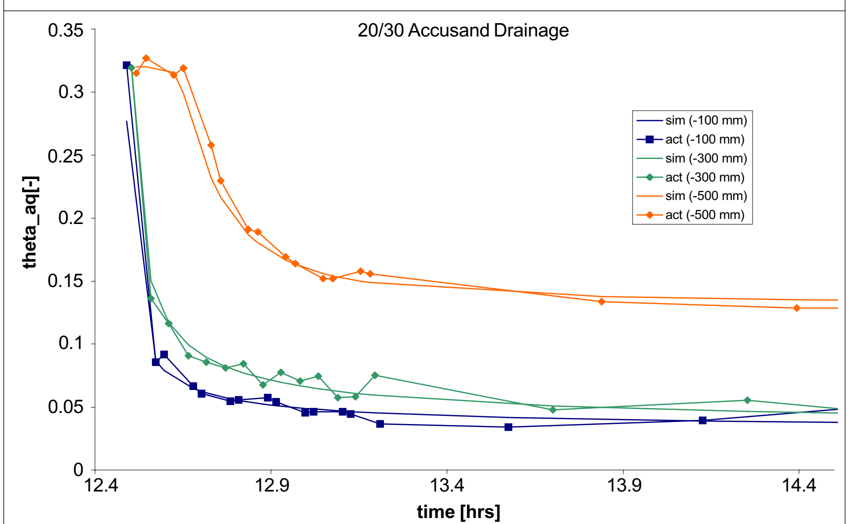

Figure 4

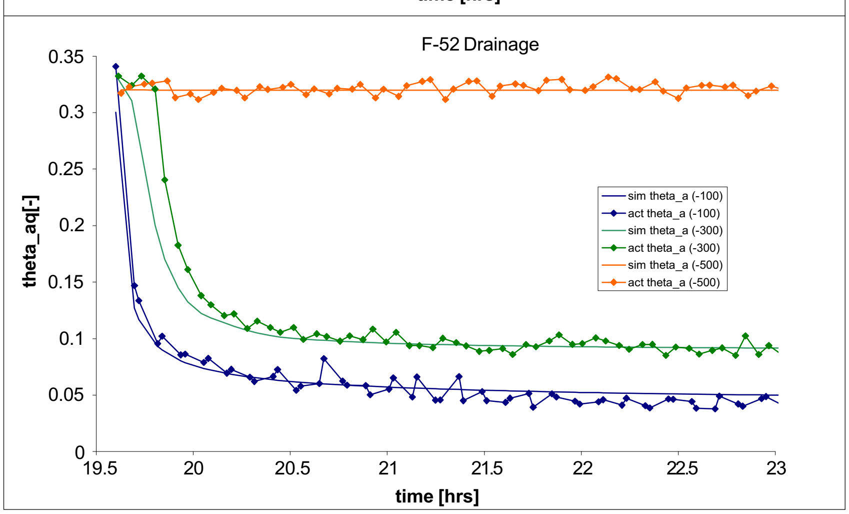

Figures 2-4. Attenuation coefficient vs. keV for Iodosoltrol and CsClwater; Modeled vs. observed water drainage data for 20/30 Accusand; Modeled vs. observed water drainage data for F-52 sand.

ate between iodosoltrol and CsClwater with attenuation data.

Comparison of the water drainage modeling results and the observed aqueous phase contents are shown in Figures 3 and 4. Although these figures only show three locations, the optimization routine was run against all the data collected.

While many of the media properties are given in Hemmer (1995) and Schroth et al. (1996), it is desirable to determine the properties specific to the packing used in this work and to compare any differences between measurement techniques (e.g., Tempe cell vs. column; dynamic vs. static). Table 3 gives the pSk parameters for the media (including values from the references), those determined during the "static" measurements, and those obtained from the water drainage modeling (termed "dynamic"). Figures 5 and 6 show the media properties and conditions for the 20/30 Accusand and F-52 sand, respectively; they include the porosity along the column, the aqueous phase content after the column had been drained (i.e., initial condition for the NAPL infiltration), and a comparison of the three pressure-saturation relations, which were obtained via the three methods discussed above.

Figures 7 and 8 show

	20/30 Accusand	F-52
static VG α (dr) [1/cm]	0.0679[1]	0.0244[2]
static VG n (dr)	13.1[1]	11.2[2]
dynamic VG α (dr) [1/cm]	0.0522	0.0249
dynamic VG n (dr)	7.9	14.9
K_s [cm/min]	8.94[1]	1.2[2]
dynamic K_s [cm/min]	3.8	2.27

Table 3. pSk parameter comparison

several NAPL break-through curves for the two experiments. As expected, the data from the 20/30 Accusand shows much more variability, due primarily to the higher media conductivity (i.e., higher NAPL flow) and the shorter counting times during the experiment.

Conclusions and Future Work

These experiments have demonstrated the effectiveness of the CASE's X-ray device to provide high-quality, dynamic phase saturation data. These data will be extremely useful for validating numerical and analytical three-phase flow models and investigating the effects of dynamics and hysteresis on pSk relations.

We are continuing to refine the path-length (phase content) estimation methods and obtaining reliable error estimates. A two-phase numerical code will be used in place of the Richards' equation code in order to obtain air and water pSk parameters. Finally, we will use the three-phase data to validate full three-phase numerical codes and to test one-dimensional analytical solutions for NAPL infiltration. ❖

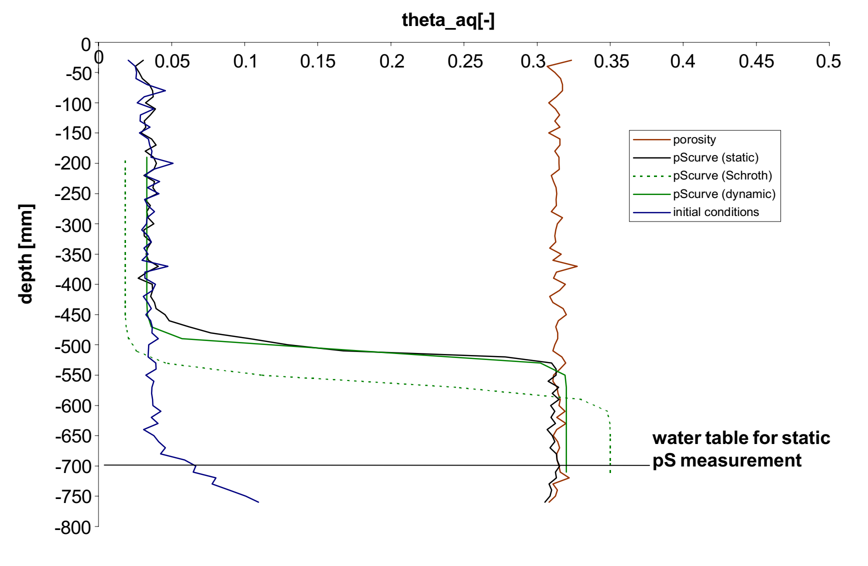

Figure 5

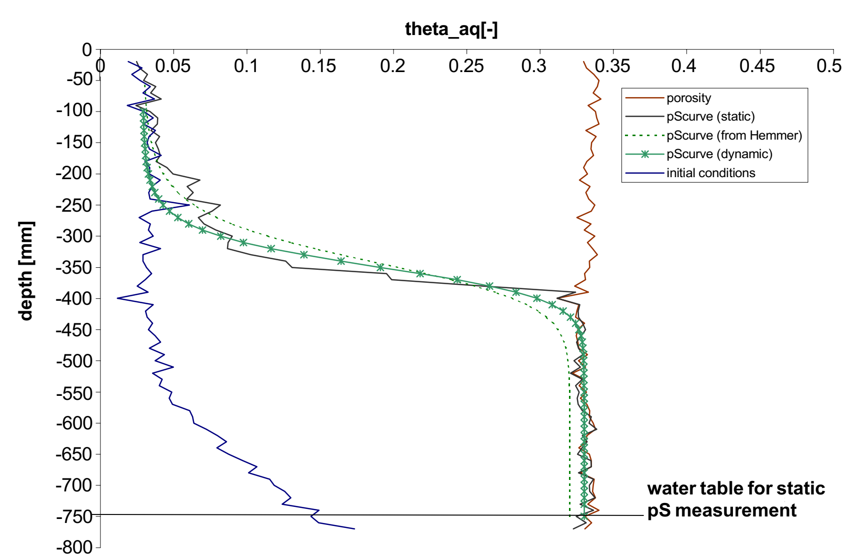

Figure 6

Figures 5-6. 20/30 Accusand Experiment; F52 Experiment.

Figure 7

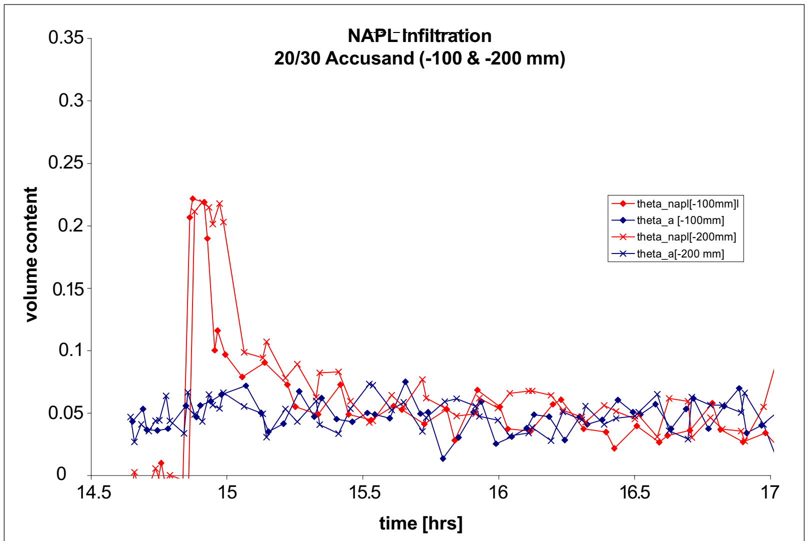

Figure 8

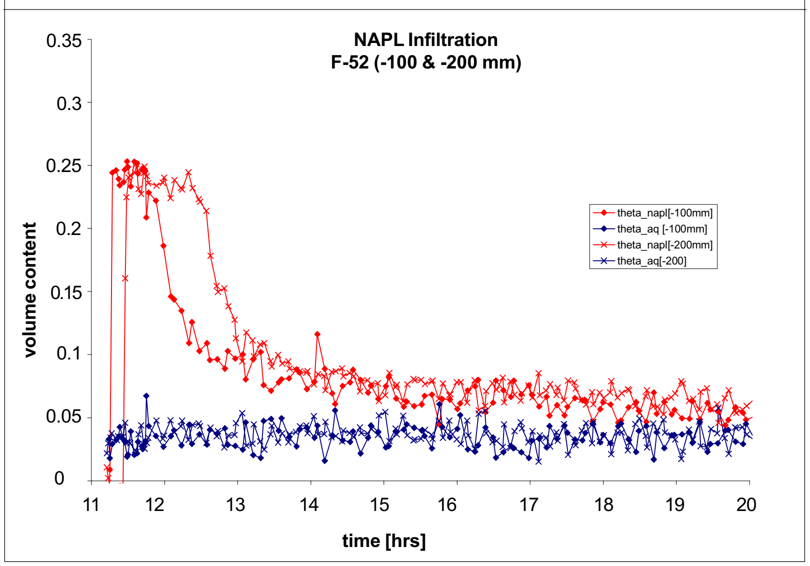

Figures 7-8. NAPL and aqueous phase contents for 20/30 Accusand; NAPL and aqueous phase contents for F-52 sand.

References

Bear, J., *Dynamics of Fluids in Porous Media*, New York, Dover, 1972.

Garbow, B. S., K. E. Hillstrom, and J. J. More, *Minpack Project*, Argonne, IL, Argonne National Lab, 1980.

Hemmer, P. M., Investigation of Methods for Determining Hydraulic Property Models for Unsaturated Flow, M.S. Thesis, University of North Carolina, Chapel Hill, NC, 1995.

Hill III, E. H., Development of Full-Spectrum X-Ray Attenuation Path-Length Estimators, *CMR Research Notes*, 1997.

Kelley, C. T., C. T. Miller, and M. D. Tocci, Termination of Newton/Chord Iterations and the Method of Lines, *SIAM Journal on Scientific Computing*, *19*(1), 280-290, 1998.

McBride, J. F., and C. T. Miller, Measurement of phase fractions in porous media by using x-rays, 1. Theoretical considerations and optimzation, *Water Resources Research*, in review, 2000a.

McBride, J. F., and C. T. Miller, Measurement of phase fractions in porous media by using x-rays, 2. Applications, *Water Resources Research*, in review, 2000b.

McBride, J. F., and C. T. Miller, Nondestructive measurement of phase fractions in multiphase porous-media experiments by using X-ray attenuation, *CMR News*, *1*(1), 10-13, 1994.

Oak, M. J., L. E. Baker, and D. C. Thomas, Three-phase relative permeability of Berea sandstone, *Journal of Petroleum Technology*, *42*(8), 1054-1061, 1990.

Schroth, M. H., S. J. Ahearn, J. S. Selker, and J. D. Istok, Characterization of Miller-similar silica sands for laboratory hydrologic studies, *Soil Science Society of American Journal 60*(5), 1331-1339, 1996.

This work was supported in part by Contract DACA39-95-K-0098 from the U.S. Army Waterways Experiment Station; Grant DAAL03-92-G- 0111 from the Army Research Office; and Grant 5 P42 ES05948 from the National Institute of Environmental Health Sciences. Computing activity was partially supported by allocations from the North Carolina Supercomputing Center.

Recent Work

I. Books

Christakos, G., *Modern Spatiotemporal Geostatistics*, Oxford University Press, New York, 2000.

Christakos, G. and D. T. Hristopulos, *Spatiotemporal Environmental Health Modelling: A Tractatus Stochasticus*, Kluwer Academic Publishers, Dordrecht, The Netherlands, 1998.

II. Book Chapters

Christakos, G., Multi-point BME space/time mapping of environmental variables, in *Computational Methods in Water Resources XII*, ed. V. N. Burganos, G. P. Karatzas, A. C. Payatakes, W. G. Gray, and G. F. Pinder, Computational Mechanics, Southampton, UK, 289-296, 1998.

Imhoff, P. T., and C. T. Miller, Nonaqueous phase liquids in the subsurface: Effects of nonaqueous-aqueous mass transfer limitations, in *Groundwater Contamination Control*, ed. K. Katsifarakis, in press, Computational Mechanics Publications, Southampton, UK, 1999.

Miller, C. T., S. N. Gleyzer, and P. T. Imhoff, Numerical modeling of NAPL dissolution fingering in porous media, in Physical Nonequilibrium in Soils: Modeling and Application, ed. H. M. Selim, and L. Ma, Ann Arbor Press, Ann Arbor, MI, 1998.

III. Journal Articles

Christakos, G., D. T. Hristopulos, and P. Bogaert, On the physical geometry hypotheses at the basis of space/time geostatistical hydrology, in press, *Advances in Water Resources*, 2000.

Christakos, G., D. T. Hristopulos, and A. Kolovos, Stochastic flowpath analysis of two-phase flow in random porous media, *SIAM Journal of Applied Mathematics*, *60*(5), 1520-1542, 2000.

Christakos, G., and A. Kolovos, A study of the spatiotemporal health impacts of ozone exposure, *Journal of Exposure Analysis and Environmental Epidemiology*, *9*(4), 322-335, 1999.

Christakos, G., and M. L. Serre, An analysis of the temperature-death rate association in the state of North Carolina, in press, *Journal of Exposure Analysis and Environmental Epidemiology*, 2000.

Christakos, G., and M. L. Serre, BME analysis of spatiotemoral particulate matter distributions in North Carolina, in press, *Atmospheric Environment*, 2000.

Christakos, G., and M. L. Serre, A spatiotemporal study of environmental exposure-health effect associations, *Journal of Exposure Analysis and Environmental Epidemiology*, *10*(2), 2000.

Farthing, M. W., and C. T. Miller, A comparison of high-resolution, finite-volume, adaptive-stencil schemes for simulating advective-dispersive transport, in press, *Advances in Water Resources*, 2000.

Gray, W. G., and C. T. Miller, Comment on "Dynamics of wetting fronts in porous media", *Physical Review E*, *61*(2), 2150-2151, 2000.

Hilpert, M., J. F. McBride, and C. T. Miller, Investigation of the residual-funicular nonwetting-phase-saturation relation, in press, *Advances in Water Resources*, 2000.

Hilpert, M., and C. T. Miller, Experimental investigation on the resonance of a liquid column in a capillary tube, *Journal of Colloid and Interface Science*, *219*, 62-68, 1999.

Hilpert, M., and C. T. Miller, Pore-morphology-based simulation of drainage in totally wetting porous media, *in review*, 2000.

Hristopulos, D. T., and G. Christakos, Practical calculation of non-Gaussian multivariate moments in BME analysis, in press, *Mathematical Geology*, 2000.

Hristopulos, D. T., and G. Christakos, Renormalization group analysis of permeability upscaling, *Stochastic Environmental Research and Risk Assessment*, *13*(1-2), 1999.

Hristopulos, D. T., G. Christakos, and M. L. Serre, Implementation of a space transform approach for solving the three-dimensional flow equation, *SIAM Journal on Scientific Computing*, *20*, 619-647, 1999.

Imhoff, P. T., C. T. Miller, and S. N. Gleyzer, The evolving interface between clean and NAPL-contaminated regions in two-dimensional porous media, in review, 2000.

Jenkins, E. W., C. T. Kelley, C. T. Miller, and C. E. Kees, An aggregation-based domain decomposition preconditioner for groundwater flow, in review, 2000.

Kees, C. E., and C. T. Miller, C++ implementations of numerical methods for solving differential-algebraic equations: Design and optimization considerations, *Association for Computing Machinery, Transactions on Mathematical Software*, *25*(4), 377-403, 1999.

McBride, J. F., and C. T. Miller, Development and application of X-ray analysis methods for multiphase porous media systems, in review, 2000.

McBride, J. F., and C. T. Miller, Measurement of phase fractions in porous media by using X-rays. 1. Theoretical considerations, in review, *Water Resources Research*, 2000.

McBride, J. F., and C. T. Miller, Measurement of phase fractions in porous media by using X-rays. 2. Applications, in review, *Water Resources Research*, 2000.

Miller, C. T., E. H. Hill III, and M. Moutier, Remediation of DNAPL-contaminated subsurface systems using density-motivated mobilization, *Environmental Science & Technology*, *34*(4), 719-724, 2000.

Miller, C. T., J. F. Kanney, and D. A. Barry, Comparison of approaches for approximating nonlinear transport and reaction problems, in review, *Advances in Water Resources*, 2000.

Serre, M. L., and G. Christakos, Modern geostatistics: Computational BME in the light of uncertain physical knowledge—the Equus Beds study, *Stochastic Environmental Research and Risk Assessment*, *13*(1), 1-26, 1999.

Tocci, M. D., C. T. Kelley, C. T. Miller, and C. E. Kees, Inexact Newton methods and the method of lines for solving Richards' equation in two space dimensions, *Computational Geosciences*, *2*(4), 291-309, 1999.

Williams, G. A., and C. T. Miller, An evaluation of temporally adaptive transformation approaches for solving Richards' equation, *Advances in Water Resources*, *22*(8), 831-840, 1999.

Williams, G. A., C. T. Miller, and C. T. Kelley, Transformation approaches for simulating flow in variably saturated porous media, *Water Resources Research*, *36*(4), 923-934, 2000.

Willson, C. S., J. L. Hall, P. T. Imhoff, and C. T. Miller, Factors affecting bank formation during surfactant-enhanced mobilization of residual NAPL, *Environmental Science & Technology*, *33*(14), 2440-2446, 1999.

Willson, C. S., O. Pau, J. A. Pedit, and C. T. Miller, Mass transfer rate limitation effects on partitioning tracer tests, in press, *Journal of Contaminant Hydrology*, 2000.

IV. Conference Proceedings

Bogaert, P., M. L. Serre, and G. Christakos, Efficient computational BME analysis of non-Gaussian data in terms of transformation functions, I, 57-62. Proceedings of the Fifth Annual Conference of the International Association for Mathematical Geology, Trodheim, Norway, 1999.

Christakos, G., D. T. Hristopulos, and M. L. Serre, BME studies of stochastic differential equations representing physical laws. Part I, I, 63-68. Proceedings of the Fifth Annual Conference of the International Association for Mathematical Geology, Trodheim, Norway, 1999.

Dalla, E., M. Hilpert, C. T. Miller, and D. Pitea, Investigation of fluid-fluid interfacial areas during primary drainage, *EOS Transactions, 81*(19), S233. American Geophysical Union Spring Meeting, Washington, DC, 30 May-3 June 2000.

Farthing, M. W., C. E. Kees, and C. T. Miller, Mixed finite element methods and higher order temporal approximations, *EOS Transactions, 81*(19), S233. American Geophysical Union Spring Meeting, Washington, DC, 30 May-3 June 2000.

Hill III, E. H., and C. T. Miller, Polyenergetic X-ray absorptiometry for porous media fluid mechanics, *EOS Transactions, 81*(19). American Geophysical Union Spring Meeting, Washington, DC, 30 May-3 June 2000.

Hill III, E. H., M. Moutier, and C. T. Miller, Remediation of DNAPL-contaminated subsurface systems using density-controlled mobilization, *EOS Transactions, 81*(19). American Geophysical Union Spring Meeting, Washington, DC, 30 May-3 June 2000.

Hilpert, M., and C. T. Miller, Pore-morphological based simulation of drainage in totally wetting porous media, *EOS Transactions, 80*(46), F396. American Geophysical Union Fall Meeting, San Francisco, CA, 13-17 December, 1999.

Hilpert, M., and C. T. Miller, Pore-morphology based calibration of a pore network model, *EOS Transactions, 81*(19), S233. American Geophysical Union Spring Meeting, Washington, DC, 30 May-3 June 2000.

Imhoff, P. T., C. T. Miller, and S. N. Gleyzer, The evolving interface between clean and NAPL-contaminated regions in two-dimensional porous media. Gordon Research Conference, Modeling of Flow in Permeable Media, Andover, NH, 6-11 August 2000.

Kees, C. E., E. W. Jenkins, C. T. Kelley, and C. T. Miller, Multilevel Schwarz preconditoners for two- and three-phase flow in porous media. 2000 Copper Mountain Conference on Iterative Methods, Copper Mountain, CO, 3-7 April 2000.

Kees, C. E., C. T. Miller, and M. W. Farthing, DAE/MOL approach for simulating multiphase flow. Fifth SIAM Conference on Mathematical and Computational Issues in the Geosciences, San Antonio, TX, 24-27 March 1999.

Kees, C. E., C. T. Miller, E. W. Jenkins, and C. T. Kelley, Two level domain decomposition techniques for multiphase flow solvers, *EOS Transactions, 81*(19), S234. American Geophysical Union Spring Meeting, Washington, DC, 30 May-3 June 2000.

Miller, C. T., Remediation of DNAPL-contaminated subsurface systems. Annual Quadrangle Conference on Environmental Sciences and Engineering, Blacksburg, VA, 13-14 February 1999.

Miller, C. T., J. F. Kanney, and D. A. Barry, Modeling reactive transport processes in porous media systems. Fifth SIAM Conference on Mathematical and Computational Issues in the Geosciences, San Antonio, TX, 24-27 March 1999.

Miller, C. T., J. F. McBride, and M. Hilpert, Pore-network modeling of the residual-funicular NAPL relation, *EOS Transactions, 80*(46), F309. American Geophysical Union Fall Meeting, San Francisco, CA, 13-17 December 1999.

Pan, C., M. Hilpert, and C. T. Miller, Pore-scale modeling of saturated permeabilities in simulated porous media, *EOS Transactions, 81*(19), S233. American Geophysical Union Spring Meeting, Washington, DC, 30 May-3 June 2000.

Pedit, J. A., C. T. Miller, R. B. Marx, and M. D. Aitken, Development of a numerical model for simulating chemotaxis in aqueous systems, *EOS Transactions, 89*(19), S250. American Geophysical Union Spring Meeting, Washington, DC, 30 May-3 June 2000.

Serre, M. L., and G. Christakos, BME studies of stochastic differential equations representing physical laws. Part II, I, 93-98. Proceedings of the Fifth Annual Conference of the International Association for Mathematical Geology, Trodheim, Norway, 1999.

Zhang, W., F. A. DiGiano, and C. T. Miller, Using sequential splitting operator methods to solve a bacterial regrowth model. 2000 Joint Conference in Water Resources Engineering and Water Resources Planning & Management, Minneapolis, MN, 30 July-2 August 2000.

CASE Directory

Faculty

George Christakos, Director	george_christakos@unc.edu	(919) 966-1767, fax (919) 966-7911
Michael Flynn	mike_flynn@unc.edu	(919) 966-3473, fax (919) 966-7911
William H. Glaze	bill_glaze@unc.edu	(919) 966-9922, fax (919) 966-9920
Markus Hilpert	markus_hilpert@unc.edu	(919) 966-0338, fax (919) 966-7911
Dionissios T. Hristopulos	dionisi_hri@unc.edu	(919) 966-7014, fax (919) 966-7911
Harvey Jeffries	harvey@unc.edu	(919) 966-7312, fax (919) 966-7911
Ross Leadbetter	mrl@stat.unc.edu	(919) 962-1040, fax (919) 962-1279
Cass T. Miller	casey_miller@unc.edu	(919) 966-2643, fax (919) 966-7911
Steven Rappaport	stephen_rappaport@unc.edu	(919) 966-5017, fax (919) 966-4711
Marc L. Serre	marc_serre@unc.edu	(919) 966-7892, fax (919) 966-7911
Richard L. Smith	rls@email.unc.edu	(919) 962-8343, fax (919) 9621279
Michael Symons	symons@bios.unc.edu	(919) 966-7266, fax (919) 966-3804
Francisco Werner	cisco@marine.unc.edu	(919) 962-0269, fax (919) 962-1254

Students

Chandra Abhishek	abhishek_chandra@.unc.edu	(919) 966-6332, fax (919) 966-4711
Rajah Augustinraj	rajah_augustinraj@unc.edu	(919) 966-6332, fax (919) 966-4711
Jose Alfaro	jose_alfaro@unc.edu	(919) 966-6332, fax (919) 966-4711
Kyung-mee Choi	kyungmee_choi@unc.edu	(919) 966-7892, fax (919) 966-7911
Matthew W. Farthing	matthew_farthing@unc.edu	(919) 966-7892, fax (919) 966-7911
Edward H. Hill III	ed_hill@unc.edu	(919) 966-6332, fax (919) 966-7911
Joseph F. Kanney	joe_kanney@unc.edu	(919) 966-7892, fax (919) 966-7911
Christopher E. Kees	chris_kees@unc.edu	(919) 966-7892, fax (919) 966-7911
Alexander Kolovos	alexander_kolovos@unc.edu	(919) 966-7892, fax (919) 966-7911
Jordan Kovitz	jkovitz@email.unc.edu	(919) 966-7892, fax (919) 966-7911
John F. McBride	john_mcbride@unc.edu	(919) 966-7892, fax (919) 966-7911
Ian Nienhueser	ian_nienhueser@unc.edu	(919) 966-6332, fax (919) 966-4711
Chongxun Pan	dpan@unc.edu	(919) 966-7892, fax (919) 966-7911
Amaury Tilmant	tilmant@email.unc.edu	(919) 966-7892, fax (919) 966-7911

Visiting Scholar

Elisa Dalla	dalla@email.unc.edu	(919) 966-7892, fax (919) 966-7911
Rubens Caldeira Monteiro	rcmonteiro@unc.edu	(919) 966-1173, fax (919) 966-7911

Research Associate

Joseph A. Pedit	joe_pedit@unc.edu	(919) 966-7892, fax (919) 966-7911

Staff

Lara Freeburg	lara_freeburg@unc.edu	(919) 966-7892, fax (919) 966-7911
Lucinda Thompson	lucinda_thompson@unc.edu	(919) 966-4175, fax (919) 966-7911

Coming in the next issue . . .

The next *CASE News* will focus on computational issues. One article compares several evolving approaches for solving a common class of transport that arises routinely in environmental modeling. The other two address pore-scale modeling based on discrete representations of the pore morphology, using the lattice-Boltzmann approach and notions from mathematical morphology.

CASE NEWS
Center for the Advanced Study of the Environment
Department of Environmental Sciences and Engineering
CB #7400, Rosenau Hall
School of Public Health
The University of North Carolina at Chapel Hill
Chapel Hill, NC 27599-7400

Nonprofit Org.
U. S. Postage
Paid
Permit No. 177
Chapel Hill, NC
27599-1110